

# A study on earthquake-resistant reinforcement using ground solidification body for underground structure

**K. Urano & T. Nishimura**

*Hazama Corporation, Tsukuba, Japan*

**Y. Adachi**

*Hazama Corporation, Tokyo, Japan*

**M. Kawamura**

*Dept. of Architecture and Civil Eng., Toyohashi University of Technology, Toyohashi, Japan*



## SUMMARY

The necessity of earthquake-resistant reinforcement for underground structure in large-scale earthquakes is rising. This paper shows a model test of the reinforcement method using the ground solidification body and its FEM analyses that were conducted to examine deformation characteristics of the reinforced underground structure and the effect of the reinforcement. The target underground structure is an RC one-box culvert and the loading tests were performed by using the 1/3 scale RC model. The reinforcement bodies made with cement and clay were situated on both sides of the structure. The effect of the reinforcement was confirmed by comparing the results of the tests with the earthquake-resistant reinforcement and without it. Elasto-plastic FEM analyses could reproduce the behaviors of the underground structure in the loading test.

*Keywords: Underground structure, Earthquake-resistant reinforcement, Ground solidification, Loading test, FEM*

## 1. INTRODUCCION

In recent years, preparing existing structures for the supposed coming large-scale earthquake has raised the necessity of the earthquake-resistant reinforcement method because the earthquake level of the seismic design was revalued. The reinforcement method for the underground structure is limited due to the construction restrictions such as site and space. As shown in **Figure 1**, the earthquake resistant reinforcement that uses the ground solidification body is reported to be effective by the numerical simulation analyses (Yamazaki et al. 2005; Urano et al. 2010).

In this paper, the model tests of the reinforcement method using the ground solidification body were conducted to examine deformation characteristics of the reinforced underground structure and the effect of the reinforcement. Moreover, the effect of reinforcement of the ground solidification body and the feature of the failure behavior are examined by the numerical simulation that uses elasto-plastic FEM analysis.

## 2. OUTLINE OF LOADING TEST

### 2.1. Test condition and loading method

#### 2.1.1. Test condition

The outline of the soil container loading test is shown in **Figure 2**. Target underground structure is RC one-box culvert and the 1/3 scale RC model (10cm in the thickness of the wall and 1m in width ×1m in height) was made for the loading tests. The main reinforcement was arranged to be D6 reinforcing bars with 150mm pitch in the RC structure model. Moreover, the ground solidification bodies of 50cm in width were set up on both sides of the structure model as reinforcement of the structure. The ground solidification body made by the high-pressure jet-grouting method was assumed, and the ground solidification bodies were made with the cement milk (Blast furnace cement) and clay called Georgia

Kaolin (Urano et al. 2011). The physical properties of the structure model and the ground solidification body are shown in **Table 1**.

The sizes of soil container used for the test were 3.0 m in width, 2.2 m in height, and 1.0 m in depth. The dry sand was filled into the container after setting the structure model. The density of the sand is  $1.70\text{g/cm}^3$ . The properties of the sand are shown in **Table 2**. The loading plates of the soil container are made of steel, and they have hinges at the lower ends. The bottom of the structure model was fixed to the concrete base with PC steel bars.

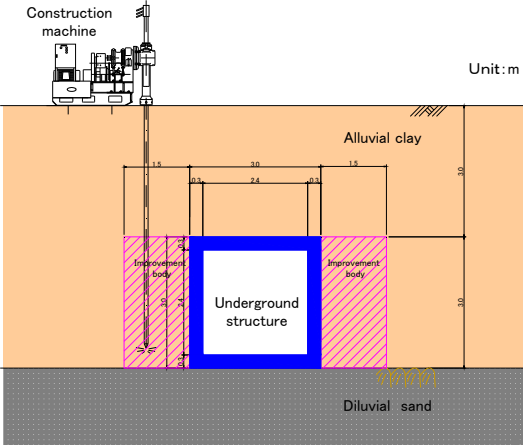


**Figure 1.** Outline of earthquake-resistant reinforcement for underground structure

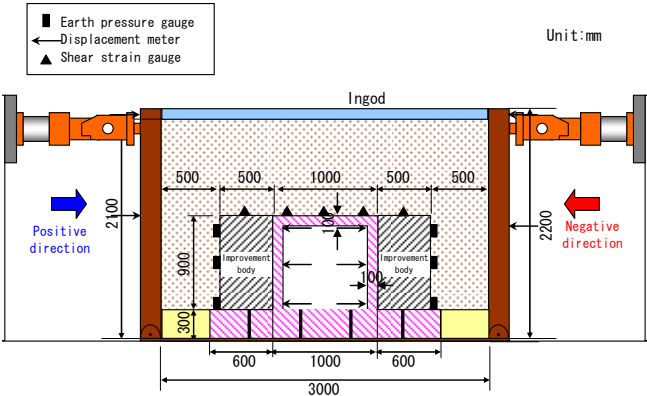


**Figure 2.** Outline of loading test



**Figure 3.** Loading test situation

**Table 1.** Physical properties of structure model and improvement body

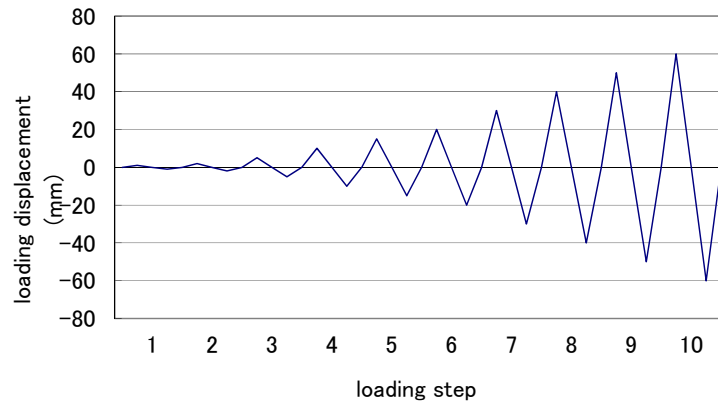
Material type	Structure model		Improvement body
	Concrete	Reinforcing bar	
Unit weight $\gamma_t$ (kN/m <sup>3</sup> )	24.0	78.5	15.0
Elastic modulus E (kN/m <sup>2</sup> )	$2.5 \times 10^7$	$2.0 \times 10^8$	$1.0 \times 10^6$
Compressive strength $\sigma_c$ (MPa)	26.8	315	1.85
Tensile strength $\sigma_t$ (MPa)	2.7	315	0.21
Poisson's ratio $\nu$	0.2	0.2	0.35

**Table 2.** Physical properties of sand

Density of soil particle $G_s$ (g/cm <sup>3</sup> )	Maximum density $\rho_{max}$ (g/cm <sup>3</sup> )	Minimum density $\rho_{min}$ (g/cm <sup>3</sup> )	Mean grain diameter $D_{50}$ (mm)	Coefficient of uniformity $U_c$
2.645	1.735	1.453	0.52	1.8

### 2.1.2. Test method

In the loading tests, the loading plates were arranged at the sides of soil container to simulate the shearing deformation by earthquake, and the loading was done horizontally by oil pressure jacks (500kN). The alternating loads by the displacement control were loaded up to 60mm as shown in **Figure 4**. The confining pressure ( $34\text{kN/m}^2$ : overburden 2m) by the soil and the steel-made ingot was made to act on the structure model and the ground solidification body. The loading tests were performed with and without the ground solidification body to compare the behaviors of the structure model. The measurements were carried out for earth pressure and shearing strain as shown in **Figure 2**.

**Figure 4.** Loading history

## 2.2. Loading test results

### 2.2.1. Load – displacement relations

The load-displacement curve of the jack is shown in **Figure 5**. At about 3 mm of relative displacement of the structure model, yield of a steel bar of the structure model occurred at lower end of the side wall. The yield of a steel bar occurred at about 20 mm loading when there was no improvement body and at about 15 mm when there were the improvement bodies. From the comparison of the maximum loads, the reinforcement effect of the improvement body was confirmed.

Moreover, the load does not fall by damage of the improvement bodies, and it is increasing gradually. Even when there is no improvement body, load is increasing with the increase in displacement.

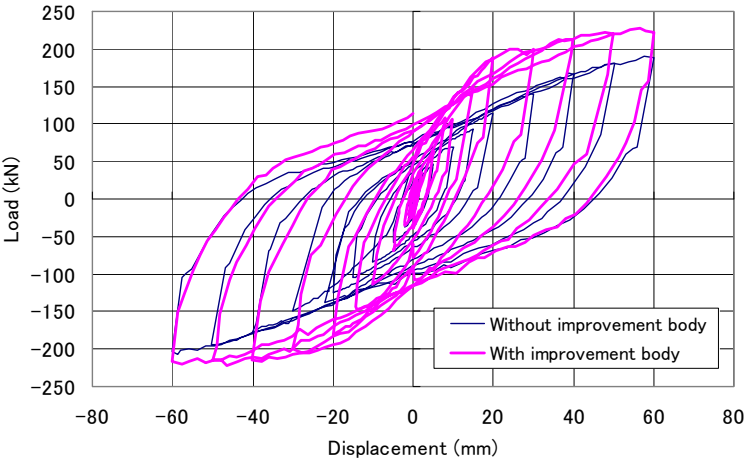


Figure 5. Load-displacement curves

2.2.2. Damage condition

The crack pattern of the improvement bodies are shown in Figure 6. The diagonal cracks occur in the improvement bodies by shear force. And crack occurs at the bottom of the improvement bodies by tension.

The crack pattern of the structure model is shown in Figure 7. The cracks without improvement body propagate from the top to the bottom of the side wall. It is because the distributed load (earth pressure) is acting to the sidewalls. On the other hand, for the case with the improvement bodies, cracks occurred in the center of the sidewall, and it is thought that this is the influence of the damage of the improvement bodies.



Figure 6. Damage condition of improvement body

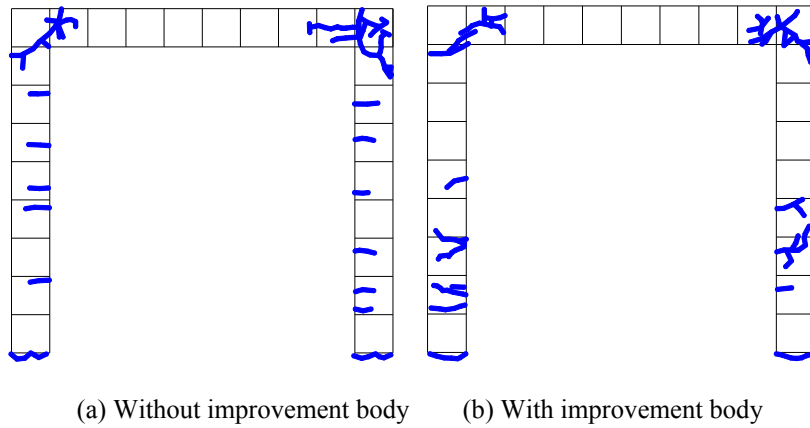


**Figure 7.** Crack pattern of structure model

### 2.2.3. Ground behavior

The increment of earth pressure that acted on the sidewall of a structure model is shown in **Figure 8**. At the left sidewall in the positive direction loading, and the right sidewall in the negative direction loading, the increment of earth pressure over  $200\text{kN/m}^2$  was measured. On the other hand, at the right sidewall in the positive direction loading, and the left sidewall in the negative direction loading, the increment of earth pressure was very small. From the above, it was confirmed the earth pressure which acts on the right and left of the structure model was different.

The distribution of maximum shear strain is shown in **figure 9**. The maximum shear strain over 5% was measured, and it was confirmed that large shear force acted on the structure model.

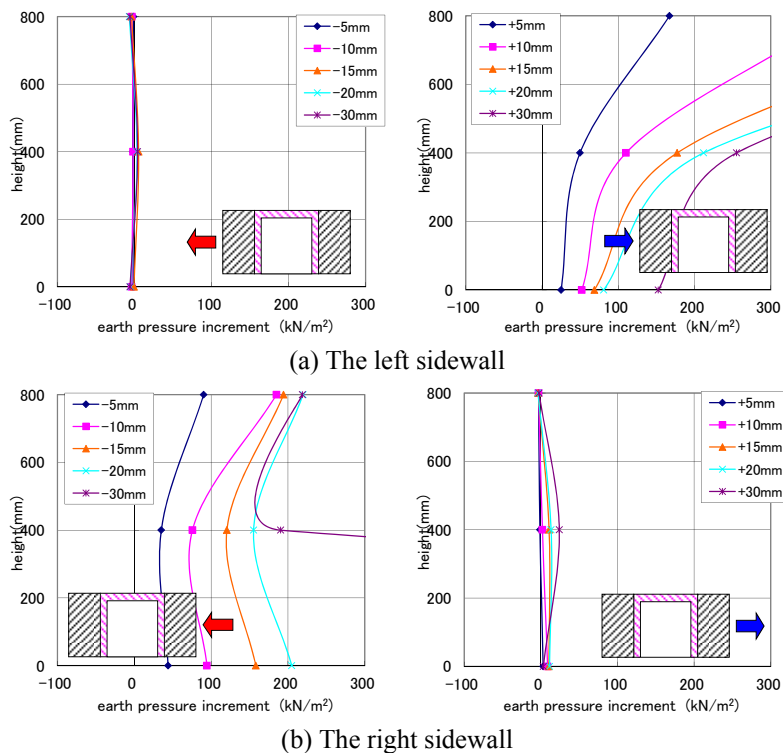


**Figure 8.** Earth pressure distribution of the sidewall (with improvement body)

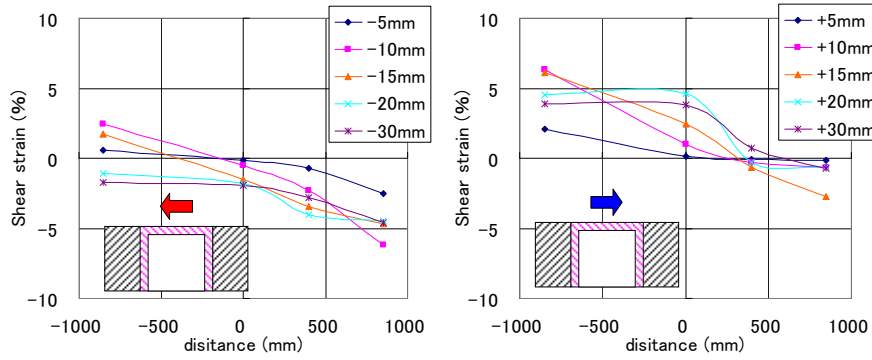


**Figure 9.** Shear strain distribution (with improvement body)

### 3. NUMERICAL SIMULATION

#### 3.1. Outline of analysis

The numerical simulation in two-dimensional FEM analysis was carried out for the soil container loading test. Because the main purpose of this analysis was reproduction of the maximum load and the mode of fracture, the loading condition in the analysis was assumed to be the monotonic loading for the positive direction.

**Figure 10** shows the FEM analytical model. Here, the structure model is consisted of beam elements. The physical properties that used in the analysis are presented in **Table 3**. The elast -plastic model that considers the tension softening (Lee and Fenves 1998; Urano et al. 2011 ) is used for the property of the reinforcing bodies. On the other hand, the Mohr-Coulomb model is used for the property of the model ground.

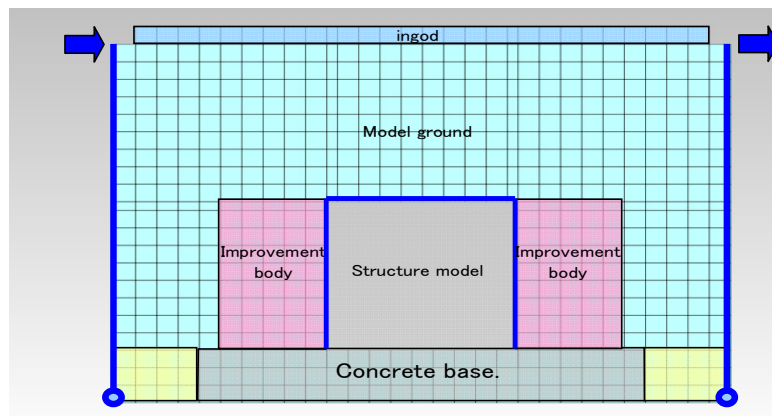


**Figure 10.** Analytical model (with improvement body)

**Table 3.** Physical properties in analysis

Type of material	Model ground	Structure model	Improvement body	Concrete base
Element	Solid element	Beam element	Solid element	Solid element
Special quality	Elasto-plastic model (Mohr-Coulomb)	Tri-linear model	Elasto-plastic model	Elasticity
Unit weight $\gamma_t$ (kN/m <sup>3</sup> )	17.0	24.0	15.0	24.0
Elastic modulus E (kN/m <sup>2</sup> )	2.6E+05	2.5E+07	1.0E+06	2.5E+07
Poisson's ratio $\nu$	0.33	0.2	0.35	0.2

### 3.2. Analytical results

#### 3.2.1. Load - displacement relations

The comparison of load–displacement curves is shown in **Figure 11**. About the case without the improvement body, the increase in the load accompanying the increase in displacement was mostly reproduced.

On the other hand, about the case with the improvement body, the behavior which the load did not increase by the damage of improvement body could be expressed by the consideration of tension softening. However, since analysis estimated the damage excessively, the load decreased.

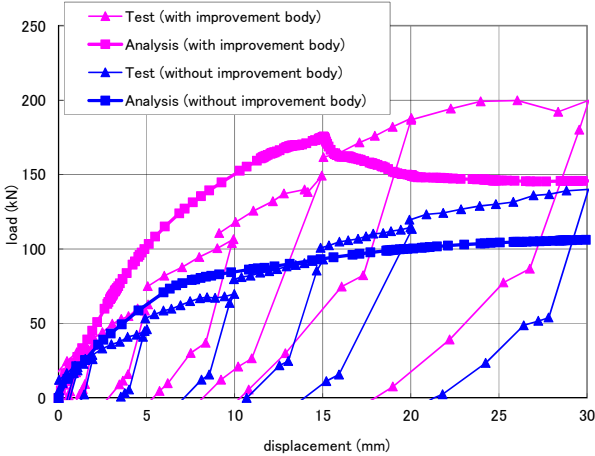


**Figure 11.** Load - soil container displacement curve

#### 3.2.2. Ground behavior and damage condition

The horizontal stress distribution without the improvement body in 20mm loading was shown in **Figure 12**. Stress states differ at the right and left of the structure model and this is the same tendency as the earth pressure distribution measured in the test. Moreover, the value of the stress in the analysis was comparable to the value of the earth pressure measured in the test.

The shear strain distribution with the improvement body in 20 mm loading is shown in **Figure 13**. The shear strain was 4-7%, and it was comparable to the value measured in the test.

The plastic strain distribution of the improvement body in 20mm loading is shown in **Figure 14**. The crack occurred in the lower part of the left improvement body and the center part of the right improvement body. It corresponds to the damage condition in the test.

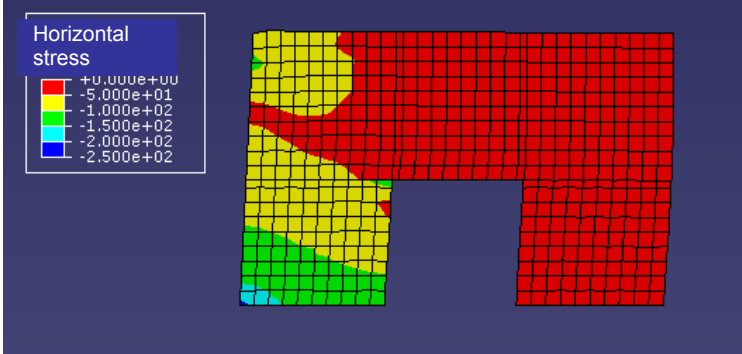


**Figure 12.** Horizontal stress distribution (Without improvement body, loading displacement 20mm)

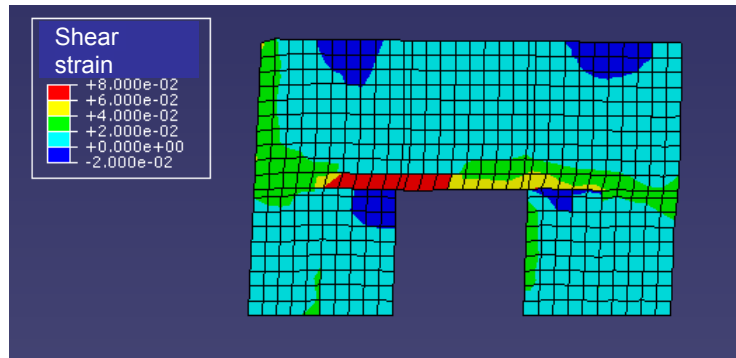


**Figure 13.** Shear strain distribution (With improvement body, loading displacement 20mm)

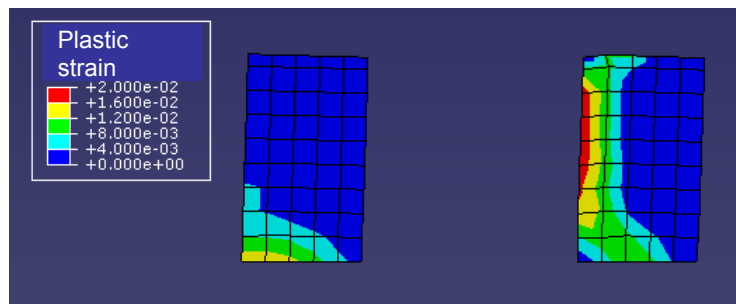


**Figure 14.** Plastic strain distribution of improvement body (Loading displacement 20mm)

#### 4. CONCLUSIONS

The soil container loading tests that used the 1/3 scale RC model of the underground structure were executed, and the effect of reinforcement of the ground solidification body and the failure behavior of the ground solidification body were confirmed. Moreover, the effect of reinforcement in the loading test and the feature of the failure behavior were reproduced by the numerical simulation.

#### REFERENCES

- Yamazaki, H., Nabetani, M., Komura, S., Higashikawa, N. and Kamegai, Y. (2005). Evaluation of anti-seismic reinforcements by soil improvement for the underground structures. *Proceedings of Japan National Conference on Geotechnical Engineering*, **40**, 2091-2092.
- Urano, K., Adachi, Y., Yamada, A., Sandanbata, I. and Kawamura, M. (2010). A study on the effect of earthquake resistant reinforcement using fiber reinforced soil improvement for underground structure: *Proceedings of Japan Society of Civil Engineers 2010 Annual Meeting*, **III-471**, 941-942.
- Urano, K., Adachi, Y., Mihara, M., Yamada, A. and Kawamura, M. (2011). Basic study on tension softening and cyclic deformation behavior of solidified body for the cohesive soil. *Journal of JSCE, Division C*, **67:4**, 500-512.
- Lee, J. and Fenves, G. L. (1998). Plastic-Damage Model for Cyclic Loading of Concrete Structures, *J. Engrg. Mech.*, ASCE, **124:8**, 892-900.